

# On formal verification of data-driven flight awareness: Leveraging the Cramér-Rao lower bound of stochastic functional time series models

Peiyuan Zhou, Saswata Paul, Airin Dutta, Carlos Varela, and Fotis Kopsaftopoulos

Rensselaer Polytechnic Institute, Troy, NY 12180, USA  
{zhoup2, pauls4, duttaa5, varelc, kopsaf}@rpi.edu

**Abstract.** This work investigates applying critically verified Cramer-Rao Lower Bound theorem, within the framework of Dynamic Data Driven Applications Systems (DDDAS), on a stochastic Vector-dependent Functionally Pooled Auto-Regressive (VFP-AR) model. (i) The VFP-AR model is identified via data obtained from wind tunnel experiments on a “fly-by-feel” wing structure under multiple flight states (i.e. angle of attack, velocity). (ii) CRLB is estimated at each true flight state reflecting the state estimation capability of the model. At the estimated flight states, corresponding CRLBs are given by testing data segment. (iii) Apart from the CRLB given by pristine data and model, CRLBs are estimated using either artificially corrupted testing data or sub-optimal models. Comparisons are made between CRLB and state estimations from corrupted and pristine conditions. (iv) The effect of corrupted data and degraded model is evaluated regarding the mechanically verified formal proof of the Cramer-Rao Lower Bound (CRLB) Theorem using Athena, which provides irrefutable guarantee of soundness as long as specified assumptions are followed. The results of the study indicate the potential of using a CRLB-based formal verification framework for state estimation via stochastic FP time series models

**Keywords:** AR models · CRLB · fly-by-feel · state awareness.

## 1 Introduction

Future intelligent aerial vehicles will be able to “feel,” “think,” and “react” in real time based on high-resolution ubiquitous sensing leading to autonomous operation based on unprecedented self-awareness and self-diagnostic capabilities. This concept falls within the core of *Dynamic Data-Driven Application Systems (DDDAS)* concept as they have to dynamically incorporate real-time data into the modeling, learning, and decision making application phases, and in reverse, steer the data measurement process based on the system’s dynamic data integration and interpretation. [3, 5, 7].

In this study, state awareness is achieved by data-driven state awareness approaches based on functionally pooled stochastic time series models and experimentally assessed on a prototype self-sensing wing structure subjected to a series of wind tunnel experiments under multiple flight states –defined by a pair

of angle of attack (AoA) and airspeed [8]. Parametric vector-dependent functionally pooled auto-regressive (VFP-AR) models are used to represent the dynamics of the wing as it undergoes different flight states. Model parameter estimation is based on a weighted least squares (WLS) approach. In addition, Cramer-Rao lower bound of VFP-AR model is formulated and introduced as means to reflect on the quality of the data and models. The formally verified CRLB theorem proved by Athena provides prior knowledge of state estimation capability based on data condition, which is checked experimentally with artificially introduced data and model abnormality. This study (i) identifies a VFP-AR model with experimental flight data for state estimation, and (ii) validates the properties and theorem of Cramer-Rao lower bound with artificially introduced data corruption and model degradation.

## 2 Functionally Pooled Time Series Models

An AR( $na$ ) model takes the following form [11]:

$$y[t] + \sum_{i=1}^{na} a_i \cdot y[t-i] = e[t] \quad e[t] \sim \text{iid} \mathcal{N}(0, \sigma_e^2) \quad (1)$$

with  $t$  designating the normalized discrete time ( $t = 1, 2, 3, \dots$  with absolute time being  $(t-1)T_s$ , where  $T_s$  stands for the sampling period),  $y[t]$  the measured vibration response signals captured by accelerometer on wing surface,  $na$  the AR polynomial order, and  $e[t]$  the stochastic model residual (one-step-ahead prediction error) sequence, that is a white (serially uncorrelated), Gaussian, zero mean with variance  $\sigma_e^2$  sequence. The symbol  $\mathcal{N}(\cdot, \cdot)$  designates Gaussian distribution with the indicated mean and variance, and iid stands for identically independently distributed.

The VFP representation combines structure dynamics captured under multiple states by AR models to be treated as one entity in model identification. Furthermore, the stochasticity in the data set is characterized as time series residual covariance and related to damage state vector via functional dependency [6, 9]. The general form of VFP-AR( $na$ ) <sub>$p$</sub>  model is given by [9]:

$$y_{\mathbf{k}}[t] = \sum_{i=1}^{na} a_i(\mathbf{k}) \cdot y_{\mathbf{k}}[t-i] + e_{\mathbf{k}}[t] \quad a_i(\mathbf{k}) = \sum_{j=1}^p a_{i,j} G_j(\mathbf{k}) \quad (2)$$

where  $na$  designating the AR order,  $p$  the number of function basis. with  $y_{\mathbf{k}}[t]$  the data under various states specified by state vector  $\mathbf{k} = [k_1, k_2, \dots, k_n]$ .  $e_{\mathbf{k}}[t]$  is the residual (one-step-ahead prediction error) sequence of the model, which is assumed a white (serially uncorrelated) zero mean sequence with variance  $\sigma_e^2(\mathbf{k})$ .  $G_j(\mathbf{k})$  is the function basis (e.g., Chebyshev, Legendre, Jacobi and etc), where the model parameters  $a_i(\mathbf{k})$  are modeled as explicit functions of the state vector  $\mathbf{k}$ . The states are estimated by minimizing model residual of VFP-AR( $na$ ) <sub>$p$</sub>  with respect to testing signal over the range of flight state vector ( $\mathbf{k}$ ).

### 2.1 Formulation of CRLB in VFP-AR model

As a minimum variance unbiased (MVU) estimator for an unbiased state estimator, CRLB informs real-time state awareness with insights into capability of

current data-driven model based on in-flight data [4]. The VFP-AR model is identified via the standard model identification process introduced by [11]. The regression form of equations (2) is obtained by parameterizing equations (2) in terms of the parameter vector ( $\boldsymbol{\theta} = [a_{1,1} \ a_{1,2} \ \dots \ a_{i,j} : \sigma_e^2(\mathbf{k})]^T$ ). Then, the parameter vector can be estimated from the measured signals via *Weighted Least Squares (WLS)* method. The CRLB of VFP-AR model is formulated for state estimator  $\hat{\mathbf{k}}$  with unknown signal,  $y_u[t]$ . Estimator  $\hat{\mathbf{k}}$  takes the form:

$$\hat{\mathbf{k}} = \arg \min_{\mathbf{k} \in \mathbf{R}^m} \sum_{i=1}^N e_u^T[t, \mathbf{k}] e_u[t, \mathbf{k}], \quad \sigma_u^2(\hat{\mathbf{k}}) = \frac{1}{N} \sum_{t=1}^N e_u[t, \hat{\mathbf{k}}] e_u^T[t, \hat{\mathbf{k}}] \quad (3)$$

where  $e_u$  is the model residual sequence and  $\sigma_u^2(\hat{\mathbf{k}})$  is the corresponding model residual variance at estimated state. Now,  $\hat{\mathbf{k}}$  is assumed to be asymptotically ( $N \rightarrow \infty$ ) Gaussian distributed with  $\hat{\mathbf{k}} \sim \mathcal{N}(\mathbf{k}, \boldsymbol{\Sigma}_{\mathbf{k}})$ . The log-likelihood function of  $\hat{\mathbf{k}}$  based on  $N$  samples of unknown signal is given by :

$$\ln \mathcal{L}(\hat{\mathbf{k}}, \sigma_u^2(\hat{\mathbf{k}})) = -\frac{N}{2} \ln(2\pi) - \frac{N}{2} \ln(\sigma_u^2) - \frac{1}{2} \sum_{t=1}^N \frac{e_u^T(\hat{\mathbf{k}}, t) e_u(\hat{\mathbf{k}}, t)}{\sigma_u^2(\hat{\mathbf{k}})} \quad (4)$$

Then, the Cramer Rao Lower bound for  $\boldsymbol{\Sigma}_{\mathbf{k}}$  is given by:

$$\boldsymbol{\Sigma}_{CRLB} = \left[ \mathbf{E} \left[ \left( \frac{\delta \ln \mathcal{L}(\mathbf{k}, \sigma_u^2)}{\delta \mathbf{k}} \right) \left( \frac{\delta \ln \mathcal{L}(\mathbf{k}, \sigma_u^2)}{\delta \mathbf{k}} \right)^T \right] \right]^{-1} \quad (5)$$

### 3 Machine-Checked Proof of the CRLB Theorem

Data corruption caused by imprecision in avionics engineering or hostile cyber activities may affect the decision chain of DDDAS systems and can lead to catastrophic errors in safety-critical aerospace systems. For this reason, it is necessary to rigorously verify all aspects of such systems to ensure that they will behave correctly within some acceptable bounds. Informal proofs of mathematical theorems can have errors [10], but formal methods allow the use of precise logical and mathematical techniques for the rigorous verification of such proofs. This is important in avionics engineering where even subtle imprecision can be catastrophic. A mechanically verified formal proof can provide an irrefutable guarantee that the property in question will be true as long as the assumptions made during proof development hold.

Athena [2] is an *interactive proof assistant* that can be used to develop and mechanically verify formal proofs of properties. It is based on *many-sorted first order logic* [12] and uses *natural deduction* [1] style proofs, which is an intuitive way of reasoning. Athena also provides a *soundness guarantee* that any proven theorem will be a logical consequence of sentences in Athena's *assumption base*, which is a set of sentences that have either been proven or asserted to

```

define CRLB-Theorem :=
  (forall theta X .
    (not
      (=
        (Random.expected (Random.pow
          (Derivative.parDifLog (Logarithm.ln (Vector.
            jointDen X theta)) theta) 2)) 0.0 ))
    ==>
    (((RealExt.pow
      (Derivative.parDif
        (Random.expected
          (Estimator.estOut (Estimator.consEst (Model.consMod theta X)))) theta)
      2)
      /
      (Random.expected (Random.pow
        (Derivative.parDifLog (Logarithm.ln (Vector.
          jointDen X theta)) theta) 2)))
    <=
    (Random.var (Estimator.estOut (Estimator.consEst (Model.consMod theta X))))))
conclude CRLB-Theorem
pick-any theta
pick-any X
assume (not (= (Random.expected (Random.pow (Derivative.parDifLog (Logarithm.ln (
  Vector.jointDen X theta)) theta) 2)) 0.0 ))
let{
  W := (Estimator.estOut (Estimator.consEst (Model.consMod theta X)));
  Y := (Derivative.parDifLog (Logarithm.ln (Vector.jointDen X theta)) theta);
  V_Y_not_zero := (not (= (Random.expected (Random.pow (Derivative.parDifLog (
    Logarithm.ln (Vector.jointDen X theta)) theta) 2)) 0.0 )));
  conn-2-Covariance-Inequality-THEOREM := (!uspec (!uspec
    Covariance-Inequality-THEOREM theta) X);
  cov-inequality-expression := (!mp conn-2-Covariance-Inequality-THEOREM
    V_Y_not_zero);
  r1 := (RealExt.pow (Derivative.parDif (Random.expected (Estimator.estOut (
    Estimator.consEst (Model.consMod theta X)))) theta) 2);
  r2 := (Random.var (Estimator.estOut (Estimator.consEst (Model.consMod theta X))));
  r3 := (Random.expected (Random.pow (Derivative.parDifLog (Logarithm.ln (Vector.
    jointDen X theta)) theta) 2));
  conn-2-swap-sides-axiom := (!uspec (!uspec (!uspec RealExt.swap-sides-axiom r1) r2
    ) r3);
  cov<=VXVY-implies-cov_by_VY<=VX := (!mp conn-2-swap-sides-axiom V_Y_not_zero)
}
(!mp cov<=VXVY-implies-cov_by_VY<=VX cov-inequality-expression)

```

Fig. 1: Specification and proof of the CRLB Theorem in Athena.

be true. We have developed a mechanically verified proof (Fig. 1) of the Cramer-Rao Lower Bound Theorem (CRLB-THEOREM) using Athena. Mathematically, CRLB-THEOREM states that:

$$\left( E \left[ \left( \frac{\partial}{\partial \theta} \log f(X; \theta) \right)^2 \right] \neq 0.0 \right) \implies \left( V[T(X)] \geq \frac{\left( \frac{\partial}{\partial \theta} E[T(X)] \right)^2}{E \left[ \left( \frac{\partial}{\partial \theta} \log f(X; \theta) \right)^2 \right]} \right)$$

where  $X = (X_1, X_2, \dots, X_N) \in R^N$  is a random vector with joint density  $f(X; \theta)$ ,  $\theta \in \Theta \subseteq R$ , and  $T(X)$  is a biased estimator of  $\theta$ . Formally specifying and proving the correctness of complex mathematical statements, such as CRLB-THEOREM, in interactive proof assistants like Athena requires access to formal constructs that are sufficiently expressive to correctly specify such statements. Furthermore, for formal reasoning about such high-level statistical properties, it is also necessary to have access to formal definitions from across mathematics, such as algebraic theory, linear algebra, measure theory, and statistics, that can support

```

datatype Estimator := (consEst Model.Model) #consEst(X ~ P_theta) -> theta_hat(X)

declare biasedEstimator : [Estimator Real] -> Boolean

declare estOut : [Estimator] -> Random.RandVar

datatype Model := (consMod Real Vector.VectRandom)

```

Fig. 2: Formal Athena constructs we have developed for the CRLB proof.

the proofs of the properties. Developing such formal constructs and definitions in a machine-readable language is a challenging task since it requires domain knowledge of all aspects of the systems that need to be specified, knowledge of formal logic and reasoning techniques, and proficiency in the machine-readable language. For this reason, we have developed an open-source proof library in Athena<sup>1</sup> that can be used for reasoning about mathematical properties of data-driven aerospace systems [13, 14]. Our specification and proof of the CRLB theorem (Fig. 1) rely on reusable formal constructs from our Athena library that are necessary for the proof to be mechanically verified. For example, we have created the Athena datatype `Estimator` to represent the domain of all estimators and a relation `biasedEstimator` over the class of all estimators to denote if an estimator is a biased estimator or not. Similarly, we have also created a datatype `Model` to denote the domain of all models. Our Athena statement of CRLB shown in Fig. 1 uses these constructs along with other constructs in our Athena library that we have developed for expressing concepts like expected value (`Random.expected`) and variance (`Random.var`) of random variables.

## 4 Experimental Results and Discussion

Structural response data is obtained through a series of wind-tunnel experiments. A “fly-by-feel” capable modular wing (NACA 4412) with internally integrated accelerometer and strain gauges is tested under multiple flight states characterized by airspeed ( $8 \sim 20 \text{ m/s}$  with  $2 \text{ m/s}$  increment) and angle of attack ( $1 \sim 15 \text{ deg}$  with  $2 \text{ deg}$  increment). Acceleration and strain signals from internally mounted ICP sensors are recorded at a sampling frequency of  $512 \text{ Hz}$  for  $128 \text{ s}$  ( $N = 65536$ ). The flight states vector  $\mathbf{k}$  is formed as  $\mathbf{k} = [k_1, k_2]$ , where  $k_1$  is air velocity and  $k_2$  is angle of attack. A data segment of  $N = 2048$  ( $t = 1 \text{ s} \sim 5 \text{ s}$ ) from each flight state is used as training data set for VFP-AR model identification. The testing data set consists of non-overlapping signal segments of  $N = 2048$  ( $t = 10 \text{ s} \sim 14 \text{ s}$ ) collected from the same flight states. Simulated data corruptions are applied to break the data normality assumption emphasized by the machine-checked CRLB theorem. “Notching” is created by uniformly replacing 10% of data with zeros replicating sensor connection faults. The CRLB of optimal model selected is estimated with respect to increasing data length from  $N = 500$  to  $N = 10000$  with 500 increment. Fig. 3 shows the CRLB converging in 2-D ellipsoid representation, which makes it easy to see the best achievable state estimation standard deviation as a function of flight parameters and flight states.

<sup>1</sup> The library can be found at <https://wcl.cs.rpi.edu/assure>

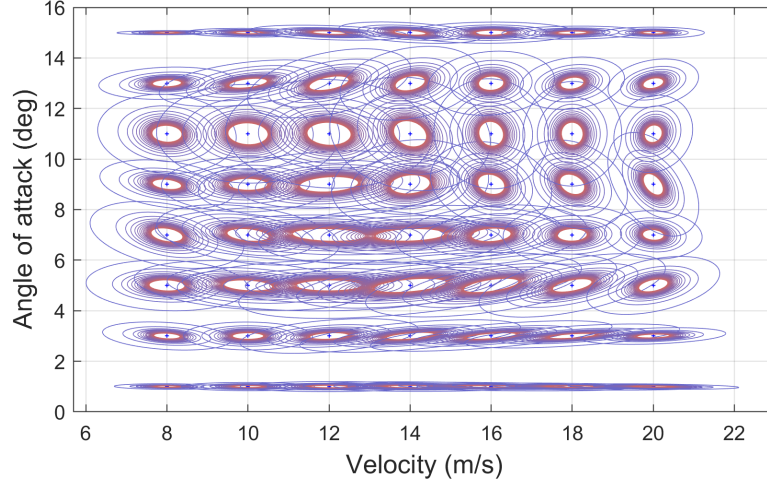


Fig. 3: CRLB estimations ellipse by 99% confidence interval assumed at exact flight state for  $VFPAR(20)_{19}$  with  $N = 500$  (blue) to  $N = 10000$  (red).

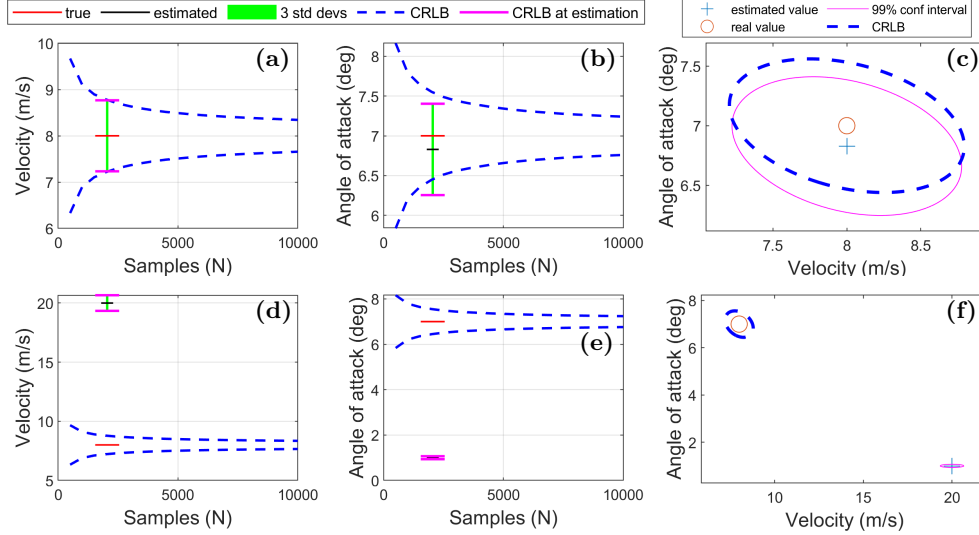


Fig. 4: Indicative CRLB estimation results comparing (a)(b)(c) uncorrupted case and (d)(e)(f) “notching” case at flight states: Velocity = 10 m/s and AoA = 1 deg. (c)(f) show CRLB in ellipsoid presentation

Aiming to evaluate the performance of CRLB under various data and model conditions, 4 different simulated data corruption and one sub-optimal model is used for flight state estimation and corresponding CRLBs at estimated flights states are calculated. The CRLBs obtained from corrupted conditions are then compared with the model residual covariance and true CRLBs where true flight states are assumed. Fig. 4(a)(b) shows the CRLB baseline using pristine data and optimal model ( $VFP - AR(20)_{19}$ ) at flight states  $\{AoA = 1 \text{ deg}, V = 10 \text{ m/s}\}$

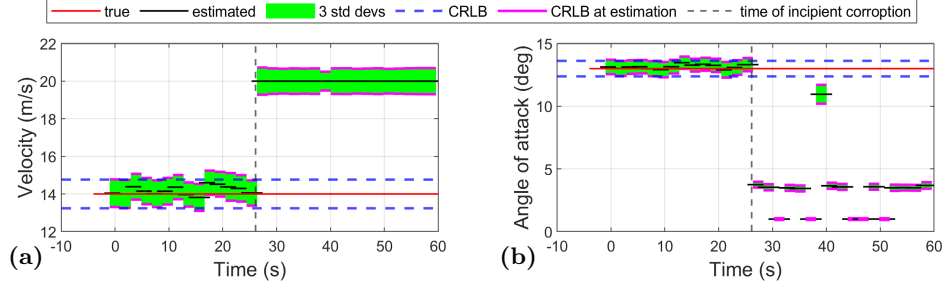


Fig. 5: Indicative CRLB real-time monitoring results based on data corrupted by zeros at  $t = 30$  s at flight states: Velocity = 14 m/s and AoA = 13 deg

and  $\{AoA = 7 \text{ deg}, V = 8 \text{ m/s}\}$ . The convergence of CRLB w.r.t increasing  $N$  is observed (dotted blue line) and the CRLBs at estimated flight states (magenta line) approximate the CRLB baseline (dotted blue line) at  $N = 2048$ . Also, CRLBs at estimations are approached by estimator standard deviation and the lower bound is followed, demonstrating the efficiency of state estimator. Fig. 4(c) shows consensus between the covariance ellipse of estimations and baseline CRLB ellipse (dotted blue line). For corrupted cases, “notching” the signals provides poor state estimation results shown in Fig. 4(d)(e). In Fig. 4(e), the CRLB of angle of attack at estimated state drops below the baseline CRLB violating the CRLB theorem.

A simulated real-time monitoring of flight state is implemented by introducing a “notching” corruption starting at  $t = 30$  s within a 64 s signal at  $\{AoA = 13 \text{ deg}, V = 14 \text{ m/s}\}$ . Test data window ( $N = 2000$ ) starts from  $t = 0$  s and advance with a  $N = 1000$  overlap until the end. Fig. 5(a)(b) shows the flight state estimation deviating from true value and estimated CRLB begin to drop lower than baseline CRLB when testing data begins to include corrupted data at  $t = 26.09375$  s. Additional results can be found in Appendix.

## 5 Conclusions

This investigating on the application of formally verified Cramer-Rao lower bound theorem in flight state awareness via VFP-AR model is presented based on data collected from a wing structure subjected to multiple flight states in wind tunnel experiments. The VFP-AR model achieves flight state awareness and provides acceptable state estimation for most test cases. The comparison between pristine CRLB and CRLB derived from corrupted data sets shows that violation of data normality asserted by formally verified CRLB theorem may causes invalidity in estimated CRLB. The case of sub-optimal model exhibits the capability of CRLB for determining the performance of a model. In general, CRLB-based formal verification framework has great potential in state estimation via stochastic FP time series models.

**Acknowledgment** This work is supported by the U.S. Air Force Office of Scientific Research (AFOSR) grant “Formal Verification of Stochastic State Awareness

for Dynamic Data-Driven Intelligent Aerospace Systems” (FA9550-19-1-0054) with Program Officer Dr. Erik Blasch.

## References

1. Arkoudas, K.: Simplifying Proofs in Fitch-Style Natural Deduction Systems. *Journal of Automated Reasoning* **34**(3), 239–294 (2005). <https://doi.org/10.1007/s10817-005-9000-3>
2. Arkoudas, K., Musser, D.: *Fundamental Proof Methods in Computer Science: A Computer-Based Approach*. MIT Press, Cambridge, MA (2017). <https://doi.org/10.1017/s1471068420000071>
3. Blasch, E., Ashdown, J., Kopsaftopoulos, F., Varela, C., Newkirk, R.: Dynamic data driven analytics for multi-domain environments. In: *Artificial Intelligence and Machine Learning for Multi-Domain Operations Applications*. vol. 11006, p. 1100604. International Society for Optics and Photonics (2019)
4. Bobrovsky, B., Zakai, M.: A lower bound on the estimation error for markov processes. *IEEE Transactions on Automatic Control* **20**(6), 785–788 (1975). <https://doi.org/10.1109/TAC.1975.1101088>
5. Breese, S., Kopsaftopoulos, F., Varela, C.: Towards proving runtime properties of data-driven systems using safety envelopes. In: *Proceedings of the 12th International Workshop on Structural Health Monitoring (IWSHM 2019)*. pp. 1748–1757. Palo Alto, CA, USA (September 2019). <https://doi.org/10.12783/shm2019/32302>
6. Kopsaftopoulos, F.P., Fassois, S.D.: Vector-dependent functionally pooled ARX models for the identification of systems under multiple operating conditions. In: *Proceedings of the 16th IFAC Symposium on System Identification, (SYSID)*. Brussels, Belgium (July 2012)
7. Kopsaftopoulos, F., Chang, F.K.: A dynamic data-driven stochastic state-awareness framework for the next generation of bio-inspired fly-by-feel aerospace vehicles. In: *Handbook of Dynamic Data Driven Applications Systems*, pp. 697–721. Springer (2018). <https://doi.org/10.1007/978-3-319-95504-9>
8. Kopsaftopoulos, F., Nardari, R., Li, Y.H., Chang, F.K.: A stochastic global identification framework for aerospace structures operating under varying flight states. *Mechanical Systems and Signal Processing* **98**, 425–447 (2018)
9. Kopsaftopoulos, F.P.: *Advanced Functional and Sequential Statistical Time Series Methods for Damage Diagnosis in Mechanical Structures*. Ph.D. thesis, Department of Mechanical Engineering & Aeronautics, University of Patras, Patras, Greece (January 2012)
10. Lamport, L.: How to Write a Proof. *The American Mathematical Monthly* **102**(7), 600–608 (1995)
11. Ljung, L.: *System Identification: Theory for the User*. Prentice–Hall, 2nd edn. (1999)
12. Manzano, M.: *Extensions of First-Order Logic*, vol. 19. Cambridge University Press, Cambridge, UK (1996)
13. Paul, S., Kopsaftopoulos, F., Patterson, S., Varela, C.A.: Dynamic Data-Driven Formal Progress Envelopes for Distributed Algorithms. In: *Dynamic Data-Driven Application Systems*. pp. 245–252 (2020)
14. Paul, S., Patterson, S., Varela, C.A.: Formal Guarantees of Timely Progress for Distributed Knowledge Propagation. In: *Formal Methods for Autonomous Systems (FMAS)*. *Electronic Proceedings in Theoretical Computer Science*, vol. 348, pp. 73–91. Open Publishing Association, The Hague, Netherlands (2021)

## A Appendix

### A.1 Additional information on machine-checked proof of the CRLB theorem

```

define Cov_Prod_Property :=
  (forall W Y . ((RealExt.pow (Random.cov W Y) 2)
    <= (* (Random.var W) (Random.var Y))))
conclude Cov_Prod_Property
  (!force Cov_Prod_Property)

```

Fig. 6: A conjecture specified in Athena, the proof for which has been forced.

We adopted a *top-down* approach of proof development in which the proofs of the higher-level theories are developed first followed by the proofs of the required lower-level theories that support them. Our proof of CRLB-THEOREM, therefore, currently relies on the following conjectures (under some assumptions) that have not yet been proven as theorems in our library:

$$\begin{aligned}
 & \text{---} \\
 & \quad (\text{Cov}[W, Y])^2 \leq V[W]V[Y] \\
 & \text{---} \\
 & \quad \text{Cov} \left[ T(X), \frac{\partial}{\partial \theta} \log f(X; \theta) \right] = \frac{\partial}{\partial \theta} E[T(X)] \\
 & \text{---} \\
 & \quad V \left[ \frac{\partial}{\partial \theta} \log f(X; \theta) \right] = E \left[ \left( \frac{\partial}{\partial \theta} \log f(X; \theta) \right)^2 \right]
 \end{aligned}$$

Currently, we have specified these conjectures in our Athena library and have “forced” their proofs to pass the mechanical verification process (Fig. 6), but we aim to develop these proofs in the future.

### A.2 State estimation error analysis

Based on  $VFP - AR(20)_{19}$ , state estimation error at each flight state varies from 1% to 20% and depends on flight states.

### A.3 Additional cases of model/data corruption

Fig. 8 shows the 1-D form of CRLB (velocity and angle of attack) converging as data length increase. In Fig. 13, additional noise to the signal affect flight state estimation, especially airspeed. In this case, it can also be observed that CRLB at estimated states drops below the true CRLB. Corrupting the data by ‘skewing’ and ‘clipping’ the signal, Fig. 11 and 12 shows good state estimation results comparable to using pristine data and no violation of true CRLB is observed. The results from sub-optimal model in Fig. 14(a)(b)(d)(e) shows less accurate flight state estimation comparing to that of optimal model. The CRLB of sub-optimal model compared to that of optimal model in Fig. 14(c)(f).

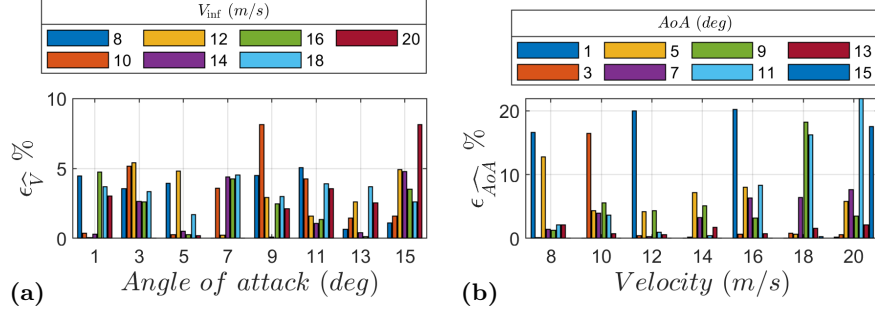


Fig. 7: Indicative VFP-AR results: state estimation error with respect to (a) AoA and (b) Velocity.

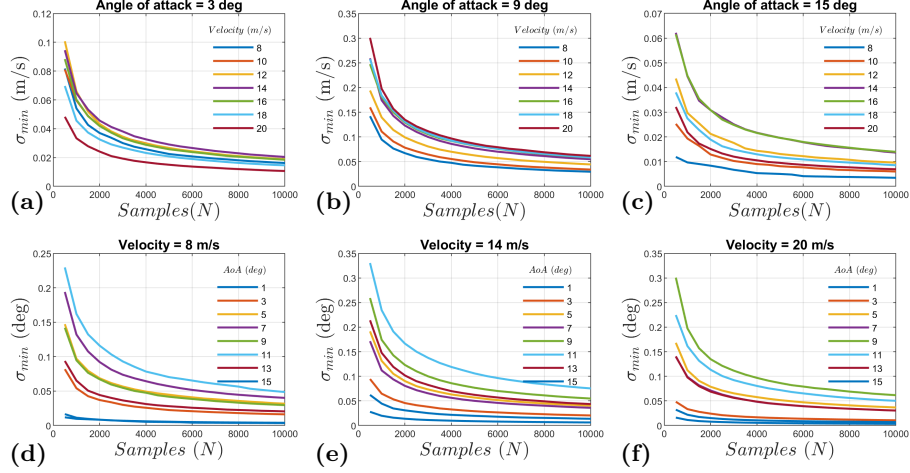


Fig. 8: Indicative CRLB estimation results based on uncorrupted data and optimal model at flight states: (a)(b)(c) fixed angle of attack of  $\{3, 9, 15\}$  deg, (d)(e)(f) fixed flow velocity of  $\{8, 14, 20\}$  m/s.

#### A.4 Real-time monitoring of flight state estimation CRLB

The real-time monitoring of flight state CRLB is implemented by introducing an persistent data corruption onset within a 64 s signal at flight states:  $\{AoA = 7 \text{ deg}, V = 8 \text{ m/s}\}$  and  $\{AoA = 13 \text{ deg}, V = 14 \text{ m/s}\}$ . Real-time test data segment ( $N = 2000$ ) is taken from the  $t = 0 \text{ s}$  with a 1000 sample overlap until the end of signal. The “notching” corruption is applied at  $t = 30 \text{ s}$ . Fig. 15(a)(b) shows that flight state estimation deviates from true value when testing data segment begins to include corrupted data at  $t = 26.09375 \text{ s}$ . Estimated CRLB begin to drop lower then pristine CRLB in Fig. 15(b) and shows jumps in estimated values.

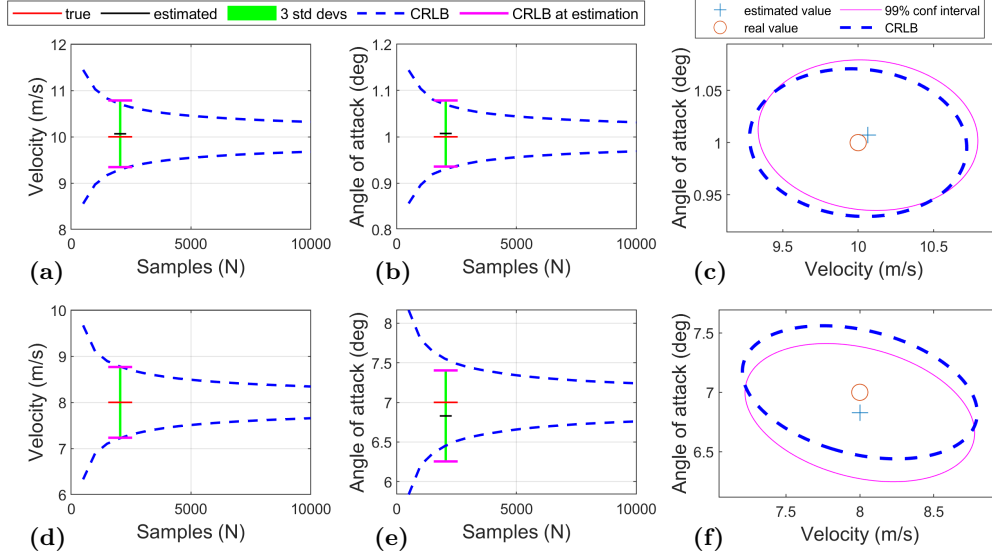


Fig. 9: Indicative CRLB estimation results based on uncorrupted data and optimal model at flight states: (a)(b) Velocity = 10  $m/s$  and AoA = 1  $deg$  , (c)(d) Velocity = 8  $m/s$  and AoA = 7  $deg$ . (c)(f) shows CRLB in ellipsoid presentation

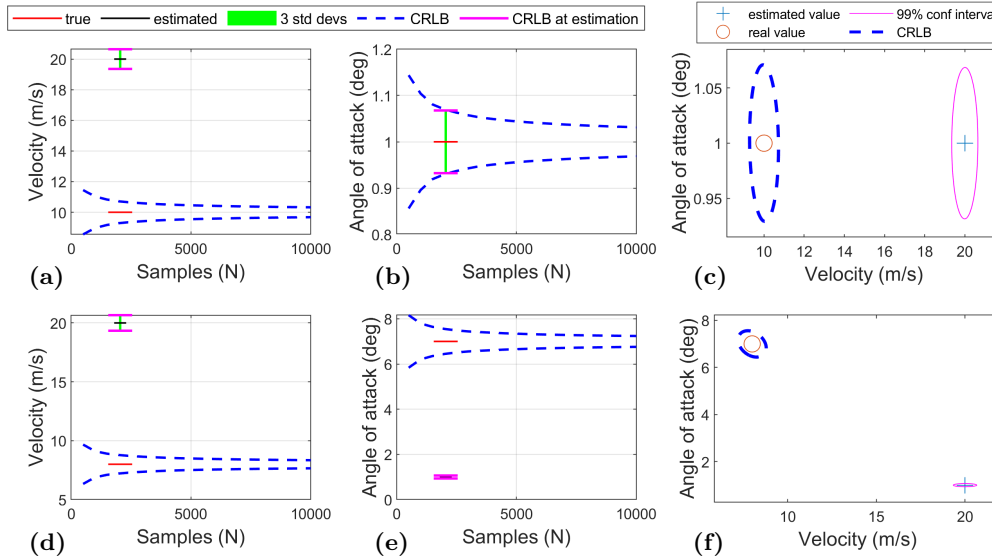


Fig. 10: Indicative CRLB estimation results based on data corrupted by 10% of zero readings at flight states: (a)(b) Velocity = 10  $m/s$  and AoA = 1  $deg$  , (c)(d) Velocity = 8  $m/s$  and AoA = 7  $deg$ . (c)(f) shows CRLB in ellipsoid presentation

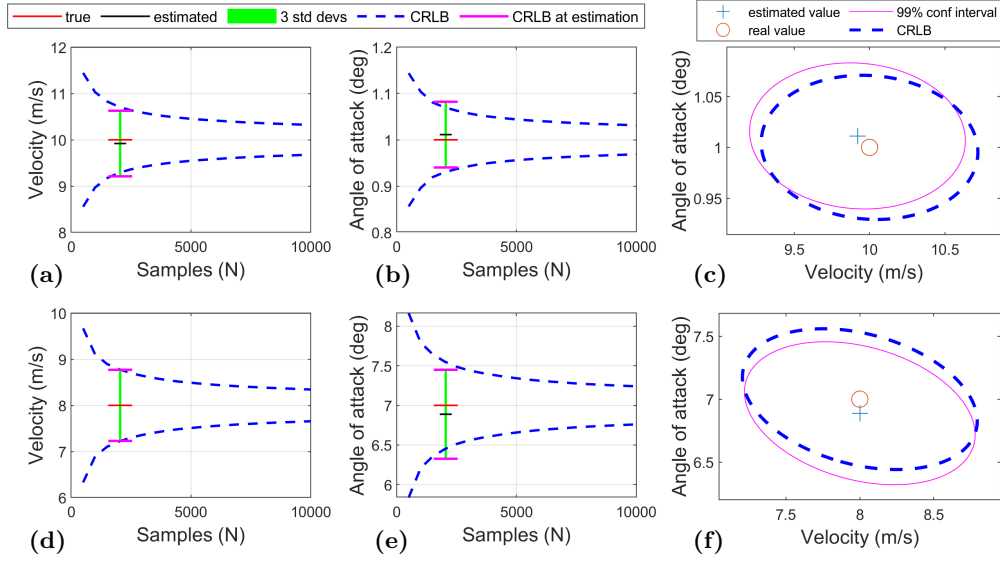


Fig. 11: Indicative CRLB estimation results based on corrupted data with 10% value compression in negative readings and 10% value expansion in positive readings at flight states: (a)(b) Velocity = 10 m/s and AoA = 1 deg, (c)(d) Velocity = 8 m/s and AoA = 7 deg. (c)(f) shows CRLB in ellipsoid presentation

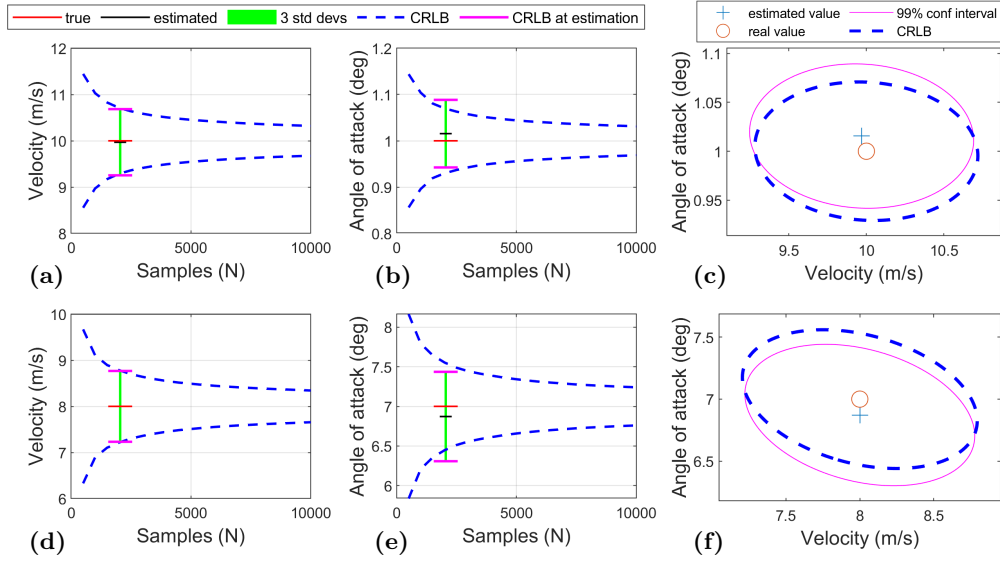


Fig. 12: Indicative CRLB estimation results based on corrupted data suffering from signal clipping that is 50% of maximum signal value at flight states: (a)(b) Velocity = 10 m/s and AoA = 1 deg, (d)(e) Velocity = 8 m/s and AoA = 7 deg. (c)(f) shows CRLB in ellipsoid presentation

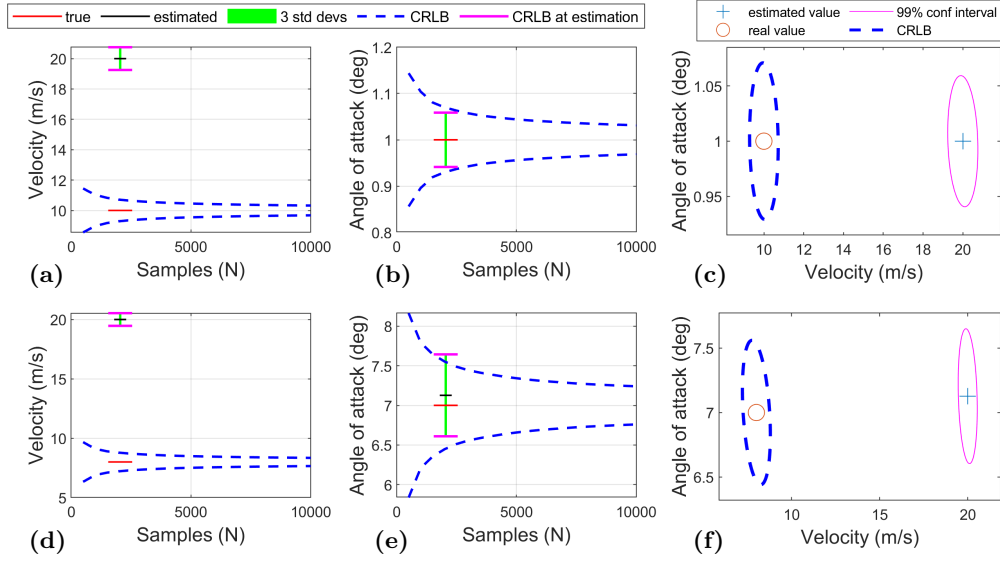


Fig. 13: Indicative CRLB estimation results based on corrupted data with and additional white noise of 10% signal standard deviation at flight states: (a)(b) Velocity = 10  $m/s$  and AoA = 1  $deg$ , (c)(d) Velocity = 8  $m/s$  and AoA = 7  $deg$ . (c)(f) shows CRLB in ellipsoid presentation

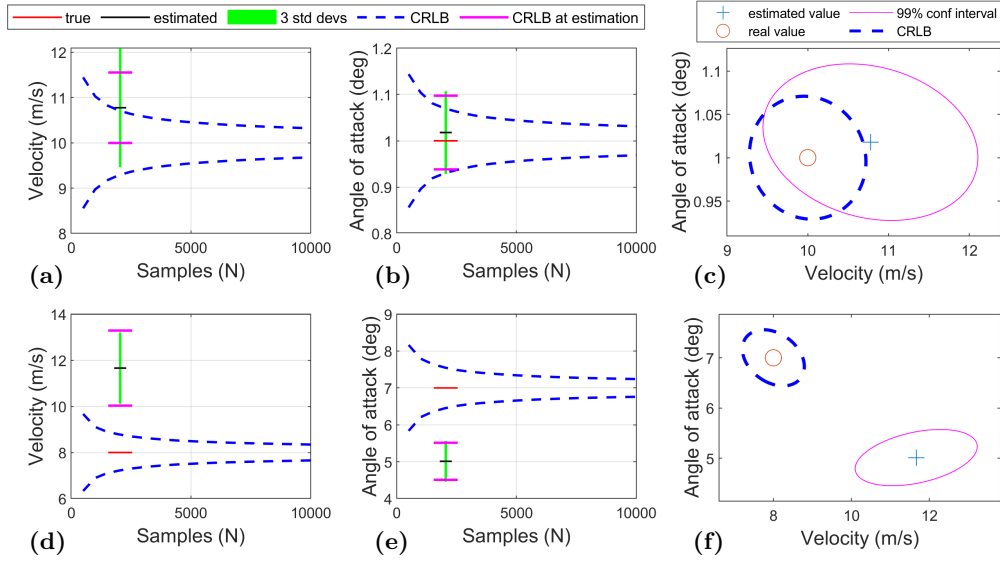


Fig. 14: Indicative CRLB estimation results based on sub-optimal model estimated with 9 VFP basis ( $p = 9$ ) at flight states: (a)(b) Velocity = 10  $m/s$  and AoA = 1  $deg$ , (c)(d) Velocity = 8  $m/s$  and AoA = 7  $deg$ . (c)(f) shows CRLB in ellipsoid presentation

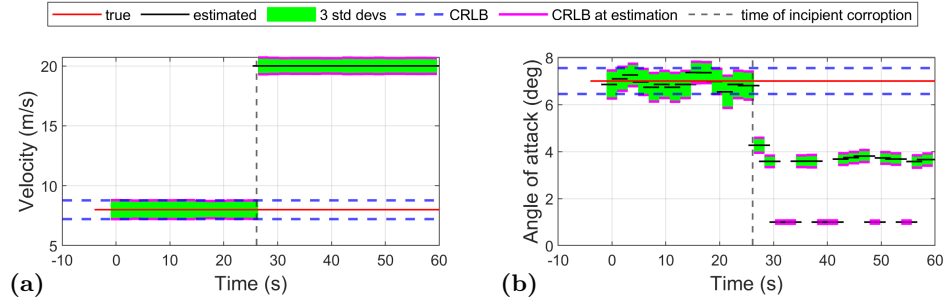


Fig. 15: Indicative CRLB real-time monitoring results based on data corrupted by zeros at  $t = 30$  s at flight states: Velocity = 8 m/s and AoA = 7 deg